Silicophytoliths from soybean plants in different growth stages of the Argentine Pampas

M. L. Benvenuto & M. L. Osterrieth

Brazilian Journal of Botany

ISSN 0100-8404

Braz. J. Bot
DOI 10.1007/s40415-015-0212-4

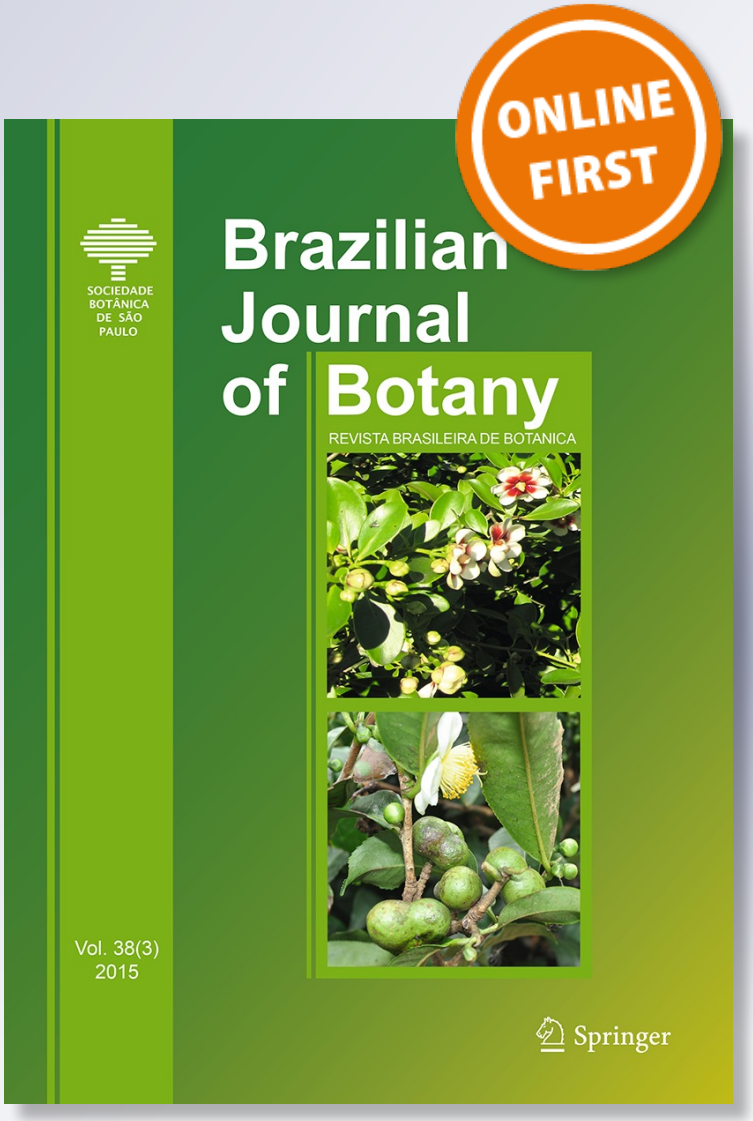

Springer

Braz. J. Bot
DOI 10.1007/s40415-015-0212-4

Silicophytoliths from soybean plants in different growth stages of the Argentine Pampas

M. L. Benvenuto[1,2] · **M. L. Osterrieth**[1,3]

Received: 22 May 2015 / Accepted: 1 September 2015

Abstract For decades, silicophytolith and silicon (Si) studies have been conducted on plant families which produce high amounts of this compound, such as horsetails, grasses, sedges, and palms. However, in recent years, studies on low silicophytolith-producing families became relevant because of the important role this compound plays in their growth. In cultivated soils from South America, research on silicophytolith production in crops and on the availability of silicon sinks is scarce. The present study is the first report of silicophytolith production in soybean plants, using staining and calcination techniques. The silicophytolith morphologies found in leaves were tabular lobate, hair bases, long and short hairs, stomatal complexes, cylindrical sulcate tracheid, elongate with fusiform edges, articulated, and orbicular cells with thickened edges silicified; in stems, branches, pods, and flowers, the silicophytoliths were orbicular and cylindrical sulcate tracheid. Throughout their growth, these soybean crops produced 1.04, 25.12, and 40.08 kg ha^{-1} of silicophytoliths in vegetative (S12), reproductive (S61), and maturity stages (S89), respectively. These results will contribute to the knowledge of the amount of silica/silicophytoliths involved in the process of Si-recycling through cultivated vegetation in fields from humid plains in medium latitude.

Keywords Argentina · Buenos aires province · Silicophytolith · Soybean

✉ M. L. Benvenuto
mlaurabenvenuto@gmail.com

[1] Instituto de Geología de Costas y del Cuaternario (IGCyC), Facultad de Ciencias Exactas y Naturales, Universidad Nacional de Mar del Plata, CC 722, Correo Central, 7600 Mar del Plata, Argentina

[2] Fondo para la Investigación Científica y Tecnológica (FONCyT), Mar del Plata, Argentina

[3] Instituto de Investigaciones Marinas y Costeras (IIMyC)-Facultad de Ciencias Exactas y Naturales, Universidad Nacional de Mar del Plata- Consejo Nacional de Investigaciones Científicas y Técnicas (CONICET), Mar del Plata, Argentina

Introduction

Biomineralizations are biogenic inorganic–organic compounds, either crystalline or amorphous, produced by organisms as a result of their metabolic activity (Lowenstam 1981; Osterrieth 2004). The most common deposits in vascular plants are silicophytoliths and calcium carbonates and oxalates (Metcalfe 1985).

Silicophytoliths, also known as biogenic opal silica, or opal phytoliths (Geis 1978; Kealhofer and Piperno 1998; Runge 1999), are composed of hydrated amorphous silica ($SiO_2 \cdot nH_2O$) which is deposited in cell walls and in extra or intracellular spaces of plant tissues (Parry and Smithson 1964; Bertoldi de Pomar 1975). The silica available as silicic acid in the soil solution is uptaken by the plant, transported by the xylem and finally it is deposited in the plant as a silicophytolith (Piperno 1988; Ma and Takahashi 2002; Exley 2009). Upon death and decay of the plants, silicophytoliths become part of the clastic materials, and they are exposed to the same weathering processes that affect soil minerals: physical breakage, chemical and biological attacks (dissolution), translocation, etc. (Osterrieth et al. 2009). These processes generate pores or cavities on the silicophytolith surface, releasing the monosilic acid. Thus, this compound can be reabsorbed by plants, it can remain in the edaphic system, be involved in the formation of secondary minerals (e.g., allophanes and amorphous

Published online: 11 September 2015

silica, and organomineral complexes), become part of the soil aggregates matrix, and/or flow into the underground water (Kelly et al. 1998; Martínez and Osterrieth 1999; Gerard et al. 2008; Borrelli et al. 2010).

For decades, silicophytolith studies have focused on palaeobotanical aspects (Twiss et al. 1969; Bertoldi de Pomar 1975; Pearsall and Trimble 1984; Piperno 1988; Osterrieth et al. 1998, 2002). These studies were conducted mainly on the plant families that produce abundant and diagnostic silicophytoliths, such as horsetails, grasses, sedges, and palms (Lovering 1959; Metcalfe 1960, 1971). However, several families which produce non-diagnostic morphotypes, but a significant amount of them, can be important for other disciplines, such as biogeochemistry and silicon cycle studies (Conley 2002; Borrelli et al. 2008). Numerous studies indicate that when silicon is readily available to plants, it plays a significant role in their growth, mineral nutrition, mechanical strength, and tolerance to biotic (e.g., plant disease and pest damage) and abiotic stresses (e.g., aluminum and heavy metals toxicity, salinity stress, drought and high temperature stress, chilling stress, mineral nutrient deficiency stress, and ultraviolet radiation) (Jones and Handreck 1967; Horiguchi 1988; Ahmad et al. 1992; Hodson and Evans 1995; Epstein 1999; Massey et al. 2007; Epstein 2009; Lux et al. 2011). However, little is known about the production of silicophytoliths and dissolved silicon fluxes in the biogeochemical cycle in cultivated fields (Guntzer et al. 2012; Keller et al. 2012; Benvenuto et al. 2013).

In South America, soybean production in the last decade grew more than twice as fast as all the other major crops, such as corn, wheat, and sunflower (FAO 2007). Argentina ranks third as soybean producer and exporter in the world (United States being first, and Brazil, second), and is the second leading exporter of soybean oil and soybean meal. The Pampean region in Argentina is an important socioeconomic sector, with soils which are among the most fertile and cultivated in the world. The grasslands developed since the Tertiary in the Pampas produced silicophytoliths, biomineralization of silt and very fine sand size, which constitute the skeletal fraction of sediments and soils (Osterrieth et al. 2014). Specifically, taphonomical, mineralogical-chemical, and chemical studies of soil solution have shown that the soil matrix is enriched in amorphous silica from the chemical degradation of silicophytoliths (Osterrieth et al. 2014). In recent years, the intensification of land use by agriculture generated a substantial loss of pelitic fractions in local soils (Osterrieth et al. 2014), causing negative effects on their physical, chemical, and biological properties, modifying silica availability, and, consequently, affecting crop growth (Keller et al. 2012). In this context, the aim of this work is to contribute to the knowledge of silicophytolith production in soybean plants cultivated in the Pampean region. Through the analysis of silicophytoliths content in soybean plants, we obtained a first approximation of the amount and type of silicophytoliths generated during the normal growth of a soybean crop, as well as the amount of silica uptake by the soil, once plants die. These results will contribute to our knowledge of the amount of silica-silicophytoliths mobilized by a soybean crop in a humid plain in the southeastern of Buenos Aires province.

Materials and methods

Study area

The southeast of Buenos Aires province (38°12′S, 57°48′W; Fig. 1) is inserted into a meadow ecosystem that has been dominated by native grasslands during late Cenozoic times (Darwin 1983). The soil in this region is Typical Argiudoll, originated from eolian sediments during the latest arid cycle of the late Pleistocene-early Holocene (SAGYP-INTA 1989). In this region the climate is mesothermic and subhumid, with little or no water deficiency (Burgos and Vidal 1951). Samplings were performed from December 2012 to March 2013. During this period, the mean precipitation values were 91.91 ± 50.709 mm, the mean maximum temperature ranged from 15.2 to 27.3 °C, and the minimum ranged from 8.7 to 14.4 °C (Meteorological Station from Mar del Plata: 876920-SAZM).

Collection of plant material and silicophytolith extraction

Three samplings were performed in December 2012, February and March 2013 to collect individuals of soybean (*Glycine max* L.) from the following growth stages, respectively: vegetative (S12), plants with trifoliolate leaf on the second node unfolded; reproductive (S61), plants in the beginning of flowering; and maturity (S89), plants with the majority of the ponds ripe, and beans dry and hard (Munger et al. 1997; Figs. 2–7). In each growth stage, nine complete specimens of soybean were randomly collected for the subsequent silicophytolith extraction in the laboratory. Moreover, the biomass of the soybean crop was estimated by extrapolation from three plots of 1 m^2. The specimens were measured (m) and each organ was carefully isolated obtaining cotyledons, leaves, stems, branches, roots, flowers, and pods. Flowers and small young leaves were analyzed together (Fig. 6), as it was impractical to separate the small leaves from the flowers. In the laboratory, each organ was subjected to a calcination technique, to obtain biogenic silica (Labouriau 1983). This

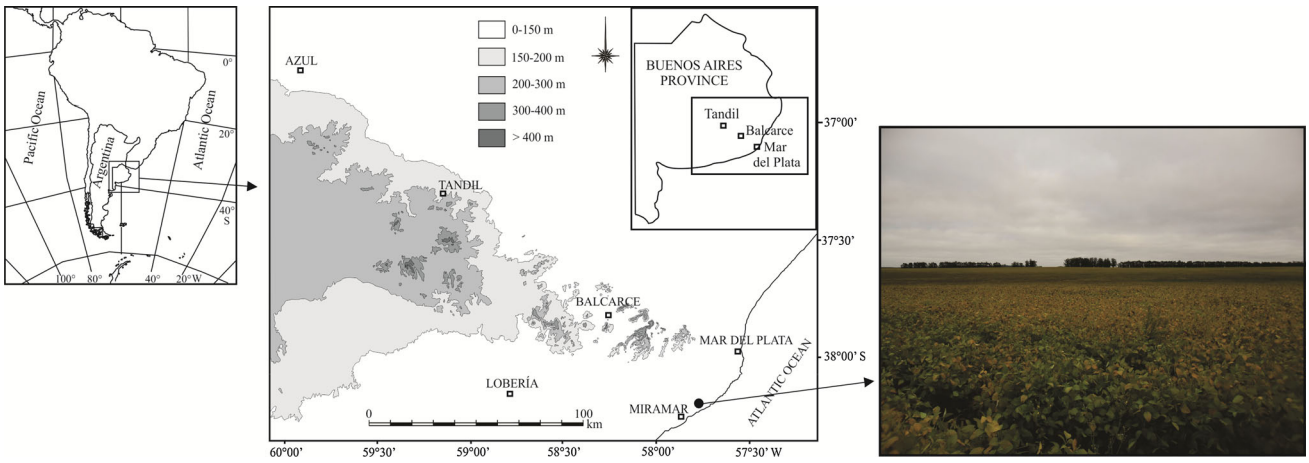

Fig. 1 Location of the study area and photograph of *Glycine max* field

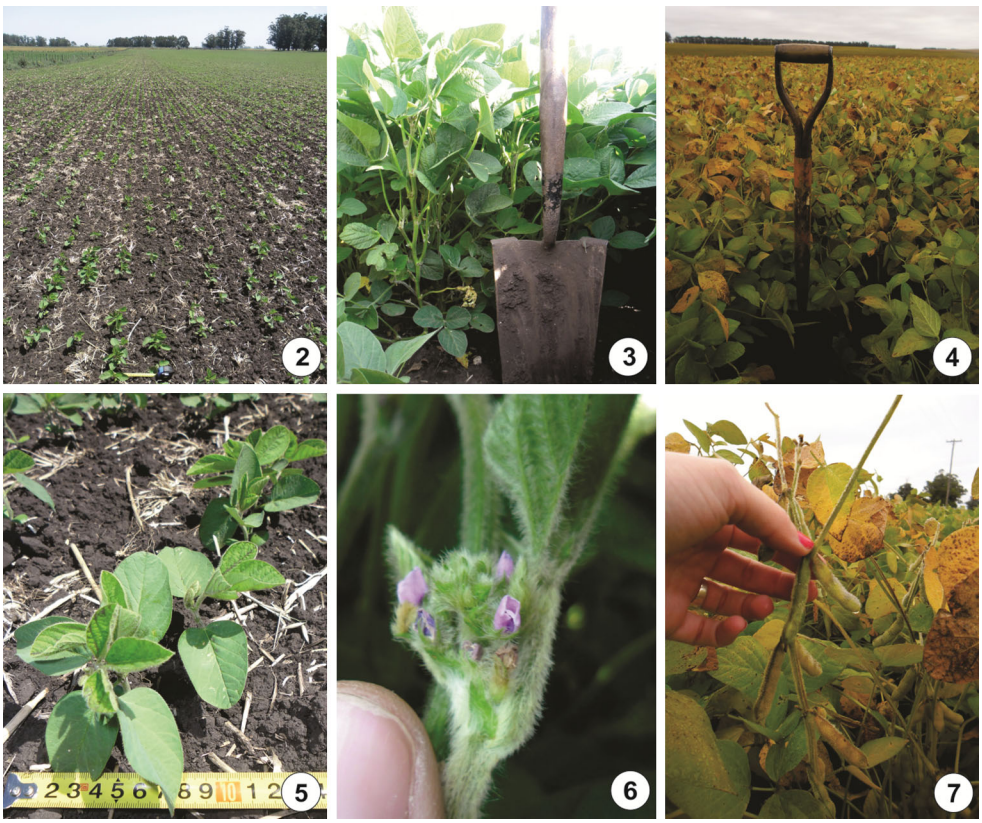

Fig. 2–7 Different growth stages of the *Glycine max* crop. *5–7* Detail of principal organs in each stage. S12, vegetative stage (*2*, *5*). S61, reproductive stage (*3*, *6*). S89, beginning of maturity stage (*4, 7*)

technique eliminates the organic matter, dissolves calcium crystals, and releases amorphous silica biomineralizations. Approximately, two plants for stage were herborized and stored in the herbarium of the Soils Geoecology Laboratory (Institute of Coasts Geology and Quaternary, Faculty of Natural Sciences, National University of Mar del Plata, Buenos Aires, Argentina).

Silicophytolith extraction

Samples were washed several times in a solution of water and detergent (commercial washing-up liquid), and rinsed with de-ionized water. Mineral matter was removed by placing the samples in an ultrasound bath (Test-Lab, Ultrasonic TB-010) for 15–20 min. Then, samples were rinsed with de-

ionized water, dried for 48 h at 60 °C, weighed (W_1), and charred at 200 °C for 2 h. After that period, samples were boiled in a 5 N HCl solution for 10 min, washed with distilled water, and filtered with ashless filter paper, until no more chloride ions were detected. Finally, the material was ignited at 760 °C for around 3 h until the ashes appeared whitish (Labouriau 1983). Ashes obtained were weighted (W_2) and silica content was calculated as a percentage of the original plant dry weight.

$$\text{Silica content}\,(\%) = (W_2/W_1) \times 100$$

Counting and microscopic observation

The ashes obtained were mounted with immersion oil and the silicophytolith morphologies were observed with a Zeiss Axiostar Plus microscope at ×400 magnification. Photographs were taken with a digital camera Cannon Powershot G10. At least two counts of 200 silicophytoliths were made for each sample and the morphologies were described. Some samples were gold-coated and observed using a scanning electron microscope (JEOL JSM-6460 LV; Japan) at National University of Mar del Plata, Buenos Aires, Argentina. The composition of the ashes was analyzed by X-ray energy dispersive spectroscopy (EDAX). The system used was an EDAX Genesis XM4-Sys 60, equipped with multichannel analyzer EDAX mod EDAM IV, Sapphire Si (lithium) detector, and super ultra-thin Window of beryl, using 15 and 25 kV accelerating voltage and EDAX Genesis version 5.11 software.

During the counting and microscopic observation, particles which had not been removed by the cleaning method were detected attached to the ashes. Therefore, some silicophytolith morphologies may not correspond to the tissue under study. Samples with a high percentage of impurities were observed under a petrographic microscope (Olympus BX51) with the aim to identify optically anisotropic and isotropic particles. Also, plant tissues were stained with phenol crystals to localize the no foreign silicophytoliths. Finally, samples were classified as sample with impurities or impurity-free samples (Table 1).

Stained with phenol crystals

Tissue were cleared with 50 % (w/v) sodium hypochlorite, dehydrated in an ethanol series, and then stained with phenol crystals. Phenol crystals stained silica in the cells with a rose color (Johansen 1940).

Estimation of silicophytolith production and input into the soil from soybean plants

Silicophytolith production in soybean plants (kg ha^{-1}) was calculated as the multiplication of (1) the biomass estimated in the field and (2) the percentage of silica content in the organs of the soybean plants corresponding to the S89 stage. All calculations were made by taking into account the mean values of the impurity-free samples.

Data analyses

Mean and standard error (SE) of amorphous silica content in each organ of soybean from different stages were calculated.

Results

Silica content and chemical nature

Silica content was observed in all soybean organs of all samples analyzed (Figs. 8–27, 28–39, 40–43). The organ that showed an increase in the dry weight percentage of silica from S12 to S89 without the presence of foreign particles in the ashes was the leaf. The weight and length of each organ analyzed and the weight of the ashes (silica content) obtained by calcination in the three growth stages are summarized in Table 1.

The analyses by X-ray energy dispersive spectroscopy (EDS) carried out on the silicophytoliths clearly showed the Si composition of these biomineralizations. However, other elements such as magnesium (Mg), aluminum (Al), potassium (K), iron (Fe), and sodium (Na) were also detected in the silicophytoliths to a lesser extent (less than 5 %) (Figs. 9, 13, 17, 21, 23, 25, 34, 38).

Silicophytolith description

The most important silicophytolith morphologies were observed in leaves, cotyledons, flowers, stems, branches, and pods. Silicophytolith assemblage in leaves was mainly represented by hair base, long and short hairs, and hair fragments (41.3 %) (Figs. 29, 32), tabular lobate (35 %) (Figs. 12, 14, 15); silica skeletons composed of thin elongated silicophytoliths and cylindrical sulcate tracheid (13.4 %) (Figs. 19, 20, 22), articulated orbicular silicophytoliths (9.1 %) (Figs. 16, 18), and stomatal complexes (1.2 %) (Fig. 35). The main morphologies observed in the cotyledons were the tabular lobate with edges thickened (61.4 %) (Figs. 8, 10, 11), and cylindrical sulcate tracheid (5.7 %). The most common morphologies observed in pods, flowers, branches, and stems were silicified hairs and hair fragments (84.2, 80.4, 14.1, and 5.8 %, respectively) (Figs. 28, 30, 31, 33), silica skeletons composed of thin elongated silicophytoliths and cylindrical sulcate tracheid (2.7, 11.2, 11.9, and 6.9 %, respectively) (Figs. 19, 20, 22), and tabular lobate silicophytoliths (less than 9 %).

Table 1 Grams of dry matter (W-organ), dry weight of ashes or silica content (W-ashes), dry weight percentage of ashes or silica content (Dry wt%), and length of plants (L-plant) from *Glycine max* organs in three growth stages (S12, S61 and S89)

Stage	Organ		Mean	SE±	Impurities
S12	Cotyledons	W-organ (g)	0.036	0.0076	
		W-ashes (g)	0.001	0.0003	✔
		Dry wt%	3.4	0.15	
S12	Root	W-organ (g)	0.068	0.0220	
		W-ashes (g)	0.003	0.0017	✔
		Dry wt%	4.4	1.92	
S12	Stem	W-organ (g)	0.064	0.0412	
		W-ashes (g)	< 0.001	0.0002	✔
		Dry wt%	1.1	1.22	
S12	Leaves	W-organ (g)	0.218	0.0636	
		W-ashes (g)	0.002	0.0006	×
		Dry wt%	0.9	0.29	
Total S12		W-plant (g)	0.333	0.1389	
		L-plant (m)	0.06	0.020	
		W-ashes (g)	0.005	0.0028	
		Dry wt%	1.5		
S61	Root	W-organ (g)	2.165	0.3397	
		W-ashes (g)	0.013	0.0034	✔
		Dry wt%	0.6	0.21	
S61	Stem	W-organ (g)	4.342	0.5884	
		W-ashes (g)	0.012	0.0045	✔
		Dry wt%	0.3	0.07	
S61	Leaves	W-organ (g)	2.610	1.3727	
		W-ashes (g)	0.046	0.0316	×
		Dry wt%	1.7	0.61	
S61	Branches	W-organ (g)	4.337	1.6518	
		W-ashes (g)	0.012	0.0038	✔
		Dry wt%	0.3	0.11	
S61	Flowers	W-organ (g)	0.307	0.0673	
		W-ashes (g)	0.003	0.0010	×
		Dry wt%	0.9	0.31	
Total S61		W-plant (g)	16.335	2.5902	
		L-plant (m)	0.58	0.056	
		W-ashes (g)	0.130	0.0397	
		Dry wt%	0.8		
S89	Root	W-organ (g)	2.277	0.4594	
		W-ashes (g)	0.017	0.0060	✔
		Dry wt%	0.8	0.26	
S89	Stem	W-organ (g)	4.494	1.0333	
		W-ashes (g)	0.011	0.0063	✔
		Dry wt%	0.2	0.12	
S89	Leaves	W-organ (g)	1.798	1.2133	
		W-ashes (g)	0.053	0.0347	×
		Dry wt%	3.1	0.66	
S89	Branches	W-organ (g)	3.369	1.4552	
		W-ashes (g)	0.024	0.0386	✔
		Dry wt%	0.8	1.45	
S89	Pods	W-organ (g)	3.195	0.9676	
		W-ashes (g)	0.012	0.0053	✔
		Dry wt%	0.4	0.16	

Table 1 continued

Stage	Organ		Mean	SE±	Impurities
Total S89		W-plant (g)	17.260	4.0306	
		L-plant (m)	0.72	0.085	
		W-ashes (g)	0.170	0.0595	
		Dry wt%	1.0		

✔ Check mark, indicates samples with presence of impurities

× Cross, indicates impurity-free sample

Although silica was detected in roots (Fig. 37), silicophytolith morphologies could not be identified (Fig. 39). In addition, an important amount of foreign particles were observed in the ashes of roots (more than 90 %), stems (89.5 %), branches (68 %), cotyledons (32.9 %), and pods (10.5 %).

The location of the silicophytolith morphologies was corroborated by the analysis of samples stained with phenol, where the main silicified areas (evidenced by a rose color) corresponded to the epidermal cells (tabular lobate silicophytoliths), parenchyma cells (orbicular silicophytoliths), and xylem and fibers (silica skeletons composed of thin elongated silicophytoliths and cylindrical sulcate tracheid).

Estimation of silicophytolith production and input into the soil from soybean plants

The biomass estimated in the field was 52 plants/m^2. The silicophytolith production in soybean plants from each stage was estimated from impurity-free samples (leaves and/or flowers, depending on the stage). The total vegetal biomass obtained in S12 was 173.32 kg ha^{-1} and the silicophytolith production was 1.04 kg ha^{-1} (leaves biomass = 113.204 kg ha^{-1}); in S61, the total vegetal biomass was 8493.94 kg ha^{-1} and the silicophytolith production was 25.12 kg ha^{-1} (leaves and flower biomass = 1516.48 kg ha^{-1}). In S89, the total vegetal biomass was 8974.99 kg ha^{-1} and the silicophytolith production was 27.61 kg ha^{-1} (leaves biomass = 934.75 kg ha^{-1}). The dry weight (g) and length (m) of the plants ranged from 0.33 g (S12) to 17.26 g (S89) and 0.06 m (S12) to 0.72 m (S89), respectively. The input of silicophytoliths to the soil at the end of the cycle (S89 stage) was 27.61 kg ha^{-1}.

Discussion and final remarks

Silicophytoliths were found in all soybean organs analyzed. Silicophytolith morphologies were not identified from ashes of roots, however, silica deposits corresponding to parenchyma and xylem tissues were observed/shown by the staining technique (Figs. 40, 41).

The highest content of silica was obtained in the leaves at S89 stage. This result was expected since this stage (corresponding to the beginning of maturity) is commonly associated with the moment of the highest silica accumulation in the life of plants (Handreck and Jones 1968). Different parts of the same plant (such as roots, stems, branches, flowers, and leaves) showed large differences in silica content; e.g., the leaves presented the highest values in S61 and S89 stages. These differences were also found in other cultivated species such as rice, oat, and wheat (Currie and Perry 2007). In soybean plants, Ma and Takahashi (2002) also reported differences in silica content, noting lower silicon content in root than in upper and lower leaves.

In the present study, petrographic microscope was used to identify the presence of foreign minerals in the samples subjected to calcination. In the same way, the counting of foreign particles in each slide was implemented, in order to estimate the percentage of impurities into the samples. Analyses by X-ray EDS were also made with the aim to corroborate the chemical nature of silicophytoliths. EDS analyses evidenced the presence of silicon as the dominant element; however, other elements such as Na, Mg, Al, K, and Fe were also detected. These elements are often associated with the plant growth (Epstein 1999), and consequently they can be incorporated into the biomineralized structures (Hodson and Sangster 1989).

The most abundant silicophytolith morphologies in leaves were derived from epidermal cell silicifications (tabular lobate, hair base, long and short hairs, and stomatal complexes). Nevertheless, the silicification process was also common in xylem (articulated cylindrical sulcate tracheid and elongate with fusiform edges), and parenchyma tissue (silicified orbicular cells with thickened edges). Orbicular and cylindrical sulcate tracheid silicophytoliths were also observed in stems, branches, pods, and flowers. In flowers, the highest percentage of silicophytoliths corresponded to silicified hairs and hair fragments produced by the young leaves, which were not separate from flowers. However, cylindrical sulcate tracheid and tabular silicophytoliths may be also assigned to flower petals since their presence was corroborated in the tissues through phenol staining (Figs. 42, 43).

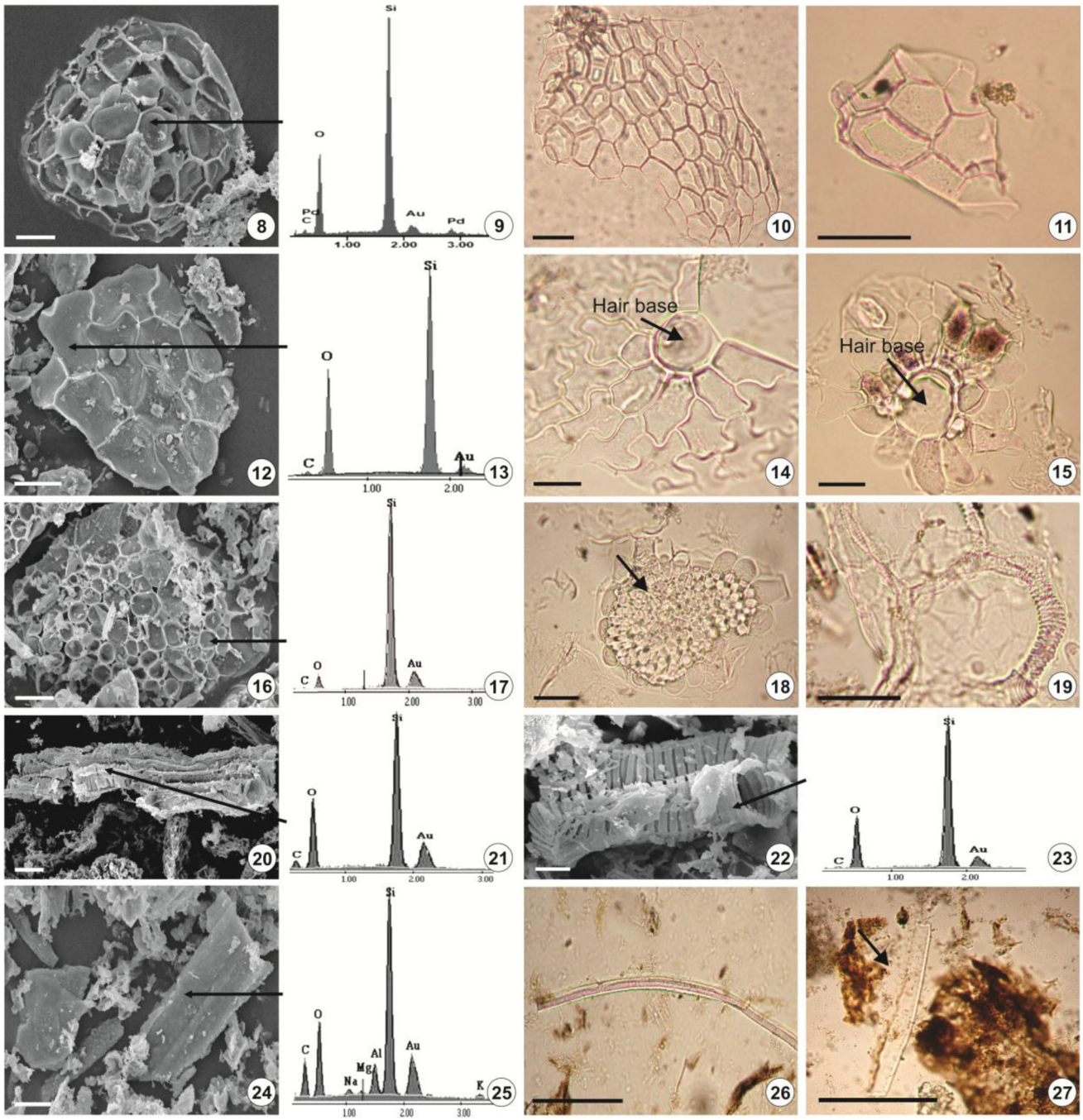

Fig. 8–27 Silicophytoliths in *Glycine max* organs observed by light and scanning electron microscopes (*8, 12, 16, 20, 22, 24*). *9, 13, 17, 21, 23, 25* EDAX analyses carried on silica morphology are indicated by the *black arrow*. *8, 10, 11* Tabular lobate silicophytoliths with edges thickened in cotyledons. *12,14, 15* Tabular lobate silicophytoliths in articulated form in leaf. *16, 18* Orbicular silicophytoliths articulated in leaves. *19, 20, 22* Cylindrical sulcate tracheid in leaf *(19, 22)* and in branches (*20*). *24, 26, 27* Elongate fragments and thin elongated silicophytoliths in stems. *Bar* 5 μm *(22)*; 10 μm *(24)*; 20 μm *(8, 10-12, 14-16, 18–20, 27)*; 50 μm (*26*)

Soybean plants increased their dry weight up to an average of 17.260 ± 4.0306 g and their length up to 0.72 ± 0.085 m. From the results obtained in the present work, we estimated a production of 27.61 kg ha^{-1} of silicophytoliths in S89 stage. Due to falling leaves in S89 (third stage), the vegetal biomass obtained for this stage was lower (934.75 kg ha^{-1}) than for the S61 stage (1356.99 kg ha^{-1}). Therefore, considering a minimum leaf biomass of 1356.99 kg ha^{-1}, the production of silicophytoliths could reach values of 40.08 kg ha^{-1}. Because soybeans seeds are the only part of the plant harvested, almost all the silicophytoliths produced by this crop will return to

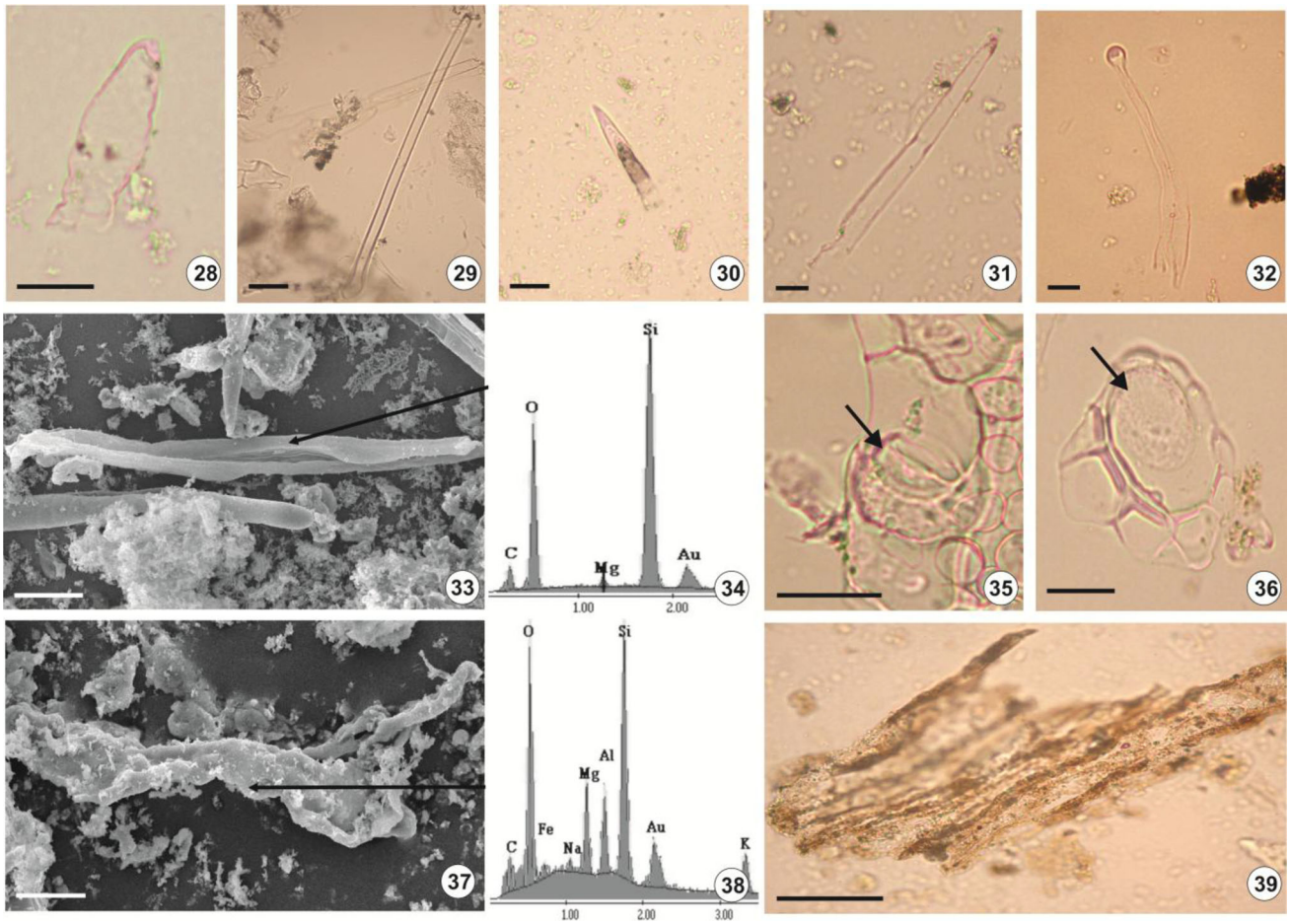

Fig. 28–39 Silicophytoliths in *Glycine max* organs observed by light and scanning electron microscopes (SEM) (*33, 37*). *34, 38* EDAX analyses carried out on silica morphology are indicated by the *black arrow*. *28–32* Silicified hairs. Silicified short hair in pods (*28*). Silicified long hair in leaves (*29*). Silicified hair fragment in stems, flowers, leaves, and pods (*30–33*, respectively). *35* Silicified stomatal complexes in leaves. *36* Silicified hair base in leaves. *37, 39* Non-identified silicophytolith morphology. *Bar* 10 μm (*37*); 20 μm (*28, 33, 35, 36, 39*); 40 μm (*29–32*)

the soil as long as farmers do not remove plant remnants from the field. Hence, at least 40.08 kg ha^{-1} of soybean silicophytoliths will be input to the soil at the end of a cycle. On the other hand and based on our results, the silica requirements for the normal development of soybean plants could be estimated. Assuming that 1356.99 kg ha^{-1} of leaf biomass from the S89 stage produces at least 40.08 kg of silicophytoliths, the production of 100 kg ha^{-1} of soybean plants would require at least 2.95 kg of silica. Similar estimations were made for rice plants, reporting that 20 kg of SiO_2 are required for a production of 100 kg of brown rice (Ma and Takahashi 2002). This value reinforces the idea that different species have different silicon requirements for their growth and development (Jones and Handreck 1965).

Silicophytoliths may be the principal immediate source and sink of silica in soil solutions, although mineral weathering is the ultimate source (Farmer et al. 2005). Scanning electron microscopy observations suggested that some weathering-like traits on the silicophytoliths surfaces might be associated to the rate of silicification reached by the opal bodies during deposition in the plant tissues. However, these surface patterns of incomplete silicification also influence the subsequent silicophytoliths weathering, prompting an easier attack on these silica bodies (Osterrieth et al. 2009). Osterrieth et al. (2009) reported that the smaller forms of silicophytoliths (< 38 mm in size) recovered from soils showed low degradation processes, probably because of the smaller surface/volume ratio. In addition, they observed that the rate of weathering was also linked to the amount of impurities present in the opal silica matrix. In consequence, grass crops such as wheat, which presents small silicophytoliths (e.g., rondels, bilobate, and short and hair cells) with an almost pure opal silica composition (M. L. Benvenuto et al., unpublished) could be considered as slow silica supplier due to their low rate of

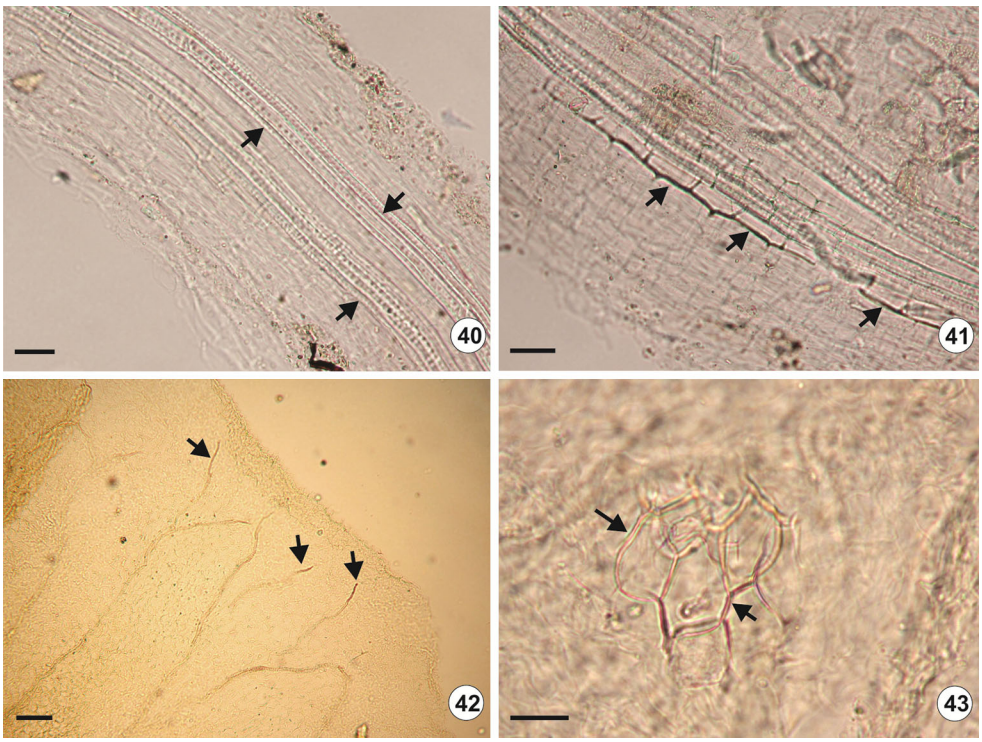

Fig. 40–43 Silicified areas from *Glycine max* roots and flowers, detected by the staining technique. *40, 41* Transverse view of the root. *42, 43* Tissue clarified from flower petals. *40, 42 Black arrows* indicate silica deposits observed in the xylem tissue. *41, 43 Black arrows* indicate silica deposits in the walls of parenchymatic cells. *Bar* 20 µm (*40, 41, 43*); 100 µm (*42*)

degradation. However, the soybean silicophytoliths which presents very different morphologies (e.g., tabular lobates, elongated cells, and elongated hair cells) and impurities in the opal silica matrix could be considered as quick silica supplier, once these are incorporated into the soil. Hence, the silicophytolith production from each cultivated species should be studied in order to increase the knowledge about the amounts and degradation rates of the silicophytolith morphologies that are involved in the process of Si-recycling through cultivated vegetation.

The present study is the first report of the presence of amorphous silica biomineralizations (silicophytoliths) in soybean plants. Both calcination and stain techniques were needed to identify the silicophytolith morphologies. Analysis of silicophytolith content allowed us to obtain a first approximation of the amount and type of silicophytoliths generated during the normal growth of a soybean crop, as well as the expected amount supplied to the soil once the plants die. However, taking into account that the availability of silicon in cultivated fields could be affected by different methods of handling, silicophytolith production from each cultivated species must be considered for correct field management.

The dynamics of soil silicon (Si) and the mechanisms that control the Si cycle are strongly linked to the incorporation of silicon by plants (Alexandre et al. 1997; Keller et al. 2012). Hence, based on the results obtained from the present work, we conclude that since soybean silicophytolith production is different from that of other important grass crops (Keller et al. 2012), crop rotation between soybean and wheat crops might be an interesting strategy to contribute to a sustainable management of silicon sources. On the other hand, the high rate of silica extraction by Si-accumulator crops, added to limited silica recycling due to total or partial export of straw from the field, could modify the availability of this element in the soil, thus interfering and affecting the proper development of the crops and their yield.

Acknowledgments The authors thank Ing. MSc. José Felix Vilá, director of Microscopy Laboratory of National University of Mar del Plata, for technical assistance on the scanning electron microscope and the Gonzalez family for providing the soybean field to perform this study. We also thank the comments and suggestions of Mariana Fernández Honaine and Macarena S. Valiñas that helped to improve our manuscript. This work was supported by Agencia Nacional de Promoción Científica y Tecnológica (PICT-2036 and PICT-1583) and Universidad Nacional de Mar del Plata (EXA 741/15).

References

Ahmad R, Zaheer S, Ismail S (1992) Role of silicon in salt tolerance of wheat (*Triticum aestivum* L.). Plant Sci 85:43–50

Alexandre A, Meunier JD, Colin F, Koud JM (1997) Plant impact on the biogeochemical cycle of silicon and related weathering processes. Geochim Cosmochin Acta 61:677–682

Benvenuto M, Osterrieth M, Fernández Honaine M (2013) Producción de Silicofitolitos en cultivos de Soja y Trigo, en el

sudeste bonaerense. In XXXIV Jornadas Argentinas de Botánica 2013 Boletín annual. Sociedad Argentina de Botánica, La Plata, p. 136

Bertoldi de Pomar H (1975) Los silicofitolitos: sinopsis de su conocimiento. Darwiniana 19:173–206

Borrelli N, Osterrieth M, Marcovecchio J (2008) Interrelations of vegetal cover, silicophytolith content and pedogenesis of Typical Argiudolls of the Pampean Plain, Argentina. Catena 75:146–153

Borrelli N, Alvarez MF, Osterrieth M, Marcovecchio J (2010) Silica content in soil solution and its relation with phytolith weathering and silica biogeochemical cycle in Typical Argiudolls of the Pampean Plain, Argentina: a preliminary study. J Soil Sediment 10:983–994

Burgos JJ, Vidal A (1951) Los climas de la República Argentina según la nueva clasificación de Thornthwaite. Meteoros 1:3–32

Conley DJ (2002) Terrestrial ecosystems and the global biogeochemical silica cycle. Glob Biogeochem Cycles 16:1121–1129

Currie H, Perry C (2007) Silica in plants: biological, biochemical and chemical studies. Ann Bot 100:1383–1389

Darwin C (1983) El viaje del Beagle. Guadarrama, Barcelona

Epstein E (1999) Silicon. Annu Rev Plant Physiol Plant Mol Biol 50:641–664

Epstein E (2009) Silicon: its manifold roles in plants. Ann Appl Biol 155:155–160

Exley C (2009) Silicon in life: whither biological silicification? In: Muller WEG, Grachev MA (eds) Biosilica in evolution, morphogenesis and nano-biotechnology. Springer, Berlin, pp 173–184

FAO (2007) Future Expansion of Soybean 2005–2014: implications for food security, sustainable rural development and agricultural policies in the Countries of Mercosur and Bolivia, synthesis document. In: Regional Office for Latin America and the Caribbean (Policy Assistance Series), Santiago, p. 53

Farmer C, Delbos E, Miller J (2005) The role of phytolith formation and dissolution in controlling concentrations of silica in soil solutions and streams. Geoderma 127:71–79

Geis JW (1978) Biogenic opal in three species of Gramineae. Ann Bot 42:1119–1129

Gerard F, Mayer KU, Hodson MJ, Ranger J (2008) Modelling the biogeochemical cycle of silicon in soils: application to a temperate forest ecosystem. Geochim Cosmochim Acta 72:741–758

Guntzer F, Keller C, Poulton PR, Mcgrath SP, Meunier J (2012) Long-term removal of wheat straw decreases soil amorphous silica at Broadbalk, Rothamsted. Plant Soil 352:173–184

Handreck KA, Jones LHP (1968) Studies of silica in the oat plant. IV. Silica content of plant parts in relation to stage of growth, supply of silica, and transpiration. Plant Soil 29:449–459

Hodson MJ, Evans DE (1995) Aluminium/silicon interactions in higher plants. J Exp Bot 46:161–171

Hodson MJ, Sangster AG (1989) Subcellular localization of mineral deposits in the roots of wheat (*Triticum aestivum* L.). Protoplasma 151:19–32

Horiguchi T (1988) Mechanism of manganese toxicity and tolerance of plant. IV. Effect of silicon on alleviation of manganese toxicity of rice plants. J Soil Sci Plant Nutr 34:65–73

Johansen DA (1940) Plant microtechnique. Mc Graw-Hill, New York

Jones LHP, Handreck KA (1965) Studies of silica in the oat plant, III: uptake of silica from soils by the plant. Plant Soil 23:79–96

Jones LHP, Handreck KA (1967) Silica in soils, plants, and animals. Adv Agron 19:107–149

Kealhofer L, Piperno DR (1998) Opal Phytoliths in Southeast Asian Flora. Smithsonian Contributions to Botany 88. Smithsonian Institution Press, Washington, DC

Keller C, Guntzer F, Barboni D, Meunier J (2012) Impact of agriculture on the Si biogeochemical cycle: input from phytolith studies. C R Geosci 344:739–746

Kelly E, Chadwick O, Hilinski T (1998) The effect of plants on mineral weathering. Biogeochemistry 42:21–53

Labouriau LG (1983) Phytolith work in Brazil: a minireview. Phytolith Newsl 2:6–10

Lovering TS (1959) Significance of accumulator plants in rock weathering. Bull Geol Soc Am 70:781–800

Lowenstam HA (1981) Minerals formed by organisms. Sci 211:1126–1131

Lux A, Martinka M, Vaculik M, White PJ (2011) Root responses to cadmium in the rhizosphere: a review. J Exp Bot 62:21–37

Ma JF, Takahashi E (2002) Soil, fertilizer, and plant silicon research in Japan. Elsevier, Amsterdam

Martínez DE, Osterrieth M (1999) Geoquímica de la sílice disuelta en el Acuífero Pampeano en la Vertiente Sudoriental de Tandilla. Hidrología Subterránea 13:241–250

Massey FP, Ennos AR, Hartley SE (2007) Herbivore specific induction of silica-based plant defences. Oecologia 152:677–683

Metcalfe CR (1960) Anatomy of monocotyledons I. Gramineae. Clarendon Press, Oxford

Metcalfe CR (1971) Anatomy of monocotyledons. V. Cyperaceae. Clarendon Press, Oxford

Metcalfe CR (1985) Anatomy of the dicotyledons II. Wood structure and conclusion of the general introduction. Clarendon Press, Oxford

Munger P, Bleiholder H, Hack H et al (1997) Phenological growth stages of the soybean plant (*Glycine max* (L.) MERR.): codification and description according to the general BBCH scale. J Agron Crop Sci 179:209–217

Osterrieth M (2004). Biominerales y Biomineralizaciones. In: Cristalografía de Suelos Resúmenes Expandidos, Sociedad Mexicana A. C. de Cristalografía, México D.F, pp 206–218

Osterrieth M, Zucol AF, Lopez de Armentia A (1998) Presencia de restos vegetales carbonizados en secuencias sedimentarias costeras del Holoceno Tardío de Mar Chiquita, Buenos Aires, Argentina. V Jornadas Geológicas Bonaerenses 2:251–255

Osterrieth M, Martínez G, Zurro D et al (2002) Procesos de formación del sitio 2 de la localidad arqueológica Amalia: evolución paleoambiental. In: Mazzanti D, Berón M, Oliva F (eds) Del mar a los salitrales: diez mil años de historia pampeana en el umbral del tercer milenio. Sociedad Argentina de Arqueología, Buenos Aires, Mar del Plata, pp 343–354

Osterrieth M, Madella M, Zurro D, Alvarez MF (2009) Taphonomical aspects of silica phytoliths in the loess sediments of the Argentinean Pampas. Quat Int 193:70–79

Osterrieth M, Benvenuto L, Alvarez M, Fernandez Honaine M (2014). Silicophytoliths: relevant buffer in the process of weathering of Typic Argiudolls, Argentinean Pampean plains. In: 9th International Meeting for Phytolith Research: toward integrative phytolith research abstracts, International Phytolith Society, Brussels, pp 42–43

Parry W, Smithson F (1964) Types of opaline silica depositions in the leaves of British grasses. Ann Bot 28:169–185

Pearsall DM, Trimble MK (1984) Identifying past agricultural activity through soil phytolith analysis: a case study from the Hawaiian Islands. J Archaeol Sci 11:119–133

Piperno DR (1988) Phytolith analysis: an archaeological and geological perspective. Academic Press, San Diego

Runge F (1999) The opal phytolith inventory of soils in Central Africa—quantities, shapes, classification, and spectra. Rev Palaeobot Palynol 107:23–53

SAGYP-INTA (1989) Mapa de suelos de la Provincia de Buenos Aires, E 1:500000. Secretaría de Agricultura, Ganadería y Pesca—Instituto Nacional de Tecnología Agropecuaria, Buenos Aires

Twiss PC, Suess E, Smith RM (1969) Morphological classification of grass phytoliths. Soil Sci Soc Am J 33:109–115